Supplement of Biogeosciences, 23, 387–398, 2026
https://doi.org/10.5194/bg-23-387-2026-supplement

Supplement of

Fucoidan carbon is stored in coastal vegetated ecosystems

Inga Hellige et al.

Correspondence to: Jan-Hendrik Hehemann (jhhehemann@marum.de)

S1 Supplementary information

S1.1 Supplementary tables

Table S1: Sediment cores taken in Germany, Malaysia and Columbia in all four ecosystems: SG (seagrass), UV (unvegetated), SM (saltmarsh) and MG (mangrove). Information on sampling location, date and time.

Country	Location	Ecosystem	Point	Longitude	Latitude	Date and time
Germany	NES	SG	P4	7.335864	53.686188	2022-08-16T08:43:00
Germany	NES	SG	P5	7.335658	53.686212	2022-08-16T08:59:00
Germany	NES	SG	P6	7.335419	53.686239	2022-08-16T09:13:00
Germany	NES	UV	P4	7.336820	53.685264	2022-08-17T07:02:00
Germany	NES	UV	P5	7.336531	53.685304	2022-08-17T07:13:00
Germany	NES	UV	P6	7.336299	53.685328	2022-08-17T07:26:00
Germany	NES	pioneer SM	P3	7.335585	53.684371	2022-08-15T10:46:00
Germany	NES	low SM	P6	7.335641	53.684276	2022-08-15T11:32:00
Germany	NES	high SM	P8	7.335455	53.683768	2022-08-15T13:59:00
Germany	NES	high SM	P9	7.335623	53.683454	2022-08-15T13:42:00
Germany	HAH	SG	P4	8.823788	54.612684	2021-11-09T09:31:03
Germany	HAH	SG	P6	8.823431	54.612663	2021-11-09T09:14:41
Germany	HAH	SG	P8	8.822986	54.612680	2021-11-09T09:01:44
Germany	HAH	UV	P4	8.811397	54.605695	2021-11-10T09:10:14
Germany	HAH	UV	P5	8.811318	54.605757	2021-11-10T09:20:28
Germany	HAH	UV	P6	8.811194	54.605855	2021-11-10T09:29:10

Germany	HAH	low SM	P5	8.825151	54.604496	2021-11-08T14:20:59
Germany	HAH	pioneer SM	P7	8.824193	54.605339	2021-11-08T13:55:06
Germany	MET	SG	P6	8.968376	54.502919	2021-11-11T09:41:19
Germany	MET	UV	P6	8.964934	54.503152	2021-11-11T12:17:11
Germany	MET	high SM	P1	8.961645	54.503247	2021-11-10T15:01:18
Germany	MET	low SM	P4	8.961963	54.503353	2021-11-10T14:30:54
Germany	SCH	SM	P4	10.024382	54.691559	2022-08-30T09:53:00
Germany	SCH	SM	P5	10.025295	54.691736	2022-08-30T09:54:00
Germany	SCH	SM	P6	10.026225	54.691997	2022-08-30T09:56:00
Germany	SCH	SM	P7	10.023244	54.692271	2022-08-30T10:43:00
Germany	WEN	SG	P5	10.287542	54.427274	2022-08-29T08:47:00
Germany	WEN	SG	P7	10.286985	54.427172	2022-08-29T08:25:00
Germany	WEN	SG	P9	10.286444	54.426960	2022-08-31T08:29:00
Germany	WEN	UV	P3	10.281737	54.425132	2022-08-26T10:31:00
Germany	WEN	UV	P5	10.281203	54.424871	2022-08-26T10:26:00
Germany	WEN	UV	P7	10.280711	54.424579	2022-08-26T10:22:00
Germany	WEN	SM	P5	10.290692	54.425844	2022-08-26T08:21:00
Germany	WEN	SM	P7	10.291283	54.426592	2022-08-26T08:16:00
Germany	WEN	SM	P9	10.291536	54.427105	2022-08-26T08:11:00
Germany	HEI	SG	P3	11.024932	54.380240	2022-08-24T10:08:00
Germany	HEI	SG	P6	11.024368	54.380322	2022-08-24T10:04:00
Germany	HEI	SG	P8	11.024125	54.380358	2022-08-24T10:02:00
Germany	HEI	UV	P3	11.023301	54.381132	2022-08-25T09:01:00
Germany	HEI	UV	P5	11.022933	54.381358	2022-08-25T09:04:00
Germany	HEI	UV	P7	11.022446	54.381428	2022-08-25T09:06:00
Germany	HEI	SM	P1	11.021790	54.377104	2022-08-23T12:11:00
Germany	HEI	SM	P3	11.020723	54.379271	2022-08-23T13:16:00

Germany	HEI	SM	P4	10.995120	54.377100	2022-08-24T07:49:00
Germany	HEI	SM	P9	10.998305	54.378869	2022-08-24T07:31:00
Malaysia	LAN	SG	P1	99.817006	6.447992	2022-09-29T00:26:00
Malaysia	LAN	SG	P3	99.817083	6.448251	2022-09-29T00:23:00
Malaysia	LAN	SG	P5	99.817260	6.448333	2022-09-29T00:19:00
Malaysia	LAN	UV	P1	99.819578	6.449959	2022-09-29T23:49:00
Malaysia	LAN	UV	P3	99.819896	6.450094	2022-09-29T23:54:00
Malaysia	LAN	UV	P5	99.820262	6.450287	2022-09-29T23:59:00
Malaysia	LAN	MG	P1	99.817696	6.448197	2022-09-24T02:47:00
Malaysia	LAN	MG	P5	99.818622	6.448140	2022-09-24T06:56:00
Malaysia	PAK	MG	P5	103.439177	4.660548	2022-10-11T04:51:00
Malaysia	PAK	MG	P9	103.439555	4.660660	2022-10-11T04:35:00
Malaysia	SET	SG	P1	102.740665	5.660896	2022-10-05T01:51:00
Malaysia	SET	SG	P2	102.740617	5.660790	2022-10-05T01:54:00
Malaysia	SET	SG	P4	102.740644	5.660663	2022-10-05T01:58:00
Malaysia	SET	UV	P1	102.740820	5.660473	2022-10-05T03:17:00
Malaysia	SET	UV	P2	102.740859	5.660461	2022-10-05T03:18:00
Malaysia	SET	UV	P3	102.740893	5.660429	2022-10-05T03:20:00
Malaysia	SET	MG	P2	102.739409	5.658089	2022-10-04T02:43:00
Malaysia	SET	MG	P5	102.739269	5.657932	2022-10-04T02:58:00
Malaysia	SET	MG	P8	102.739227	5.657740	2022-10-04T02:23:00
Malaysia	SET	SM	P1	102.743881	5.658787	2022-10-09T03:01:00
Malaysia	SET	SM	P3	102.744144	5.658643	2022-10-09T02:58:00
Malaysia	SET	SM	P5	102.744319	5.658541	2022-10-09T02:55:00
Columbia	1	SG	P3	-75.681974	10.136862	2022-05-03T16:47:00
Columbia	1	SG	P4	-75.681995	10.136855	2022-05-03T16:48:00
Columbia	1	SG	P8	-75.682115	10.137064	2022-05-03T16:53:00

Columbia	1	UV	P2	-75.682109	10.137113	2022-05-03T16:57:00
Columbia	1	UV	P3	-75.682165	10.137153	2022-05-03T16:56:00
Columbia	1	UV	P4	-75.682178	10.137119	2022-05-03T16:55:00
Columbia	1	MG	P7	-75.682718	10.136688	2022-05-01T14:44:00
Columbia	1	MG	P8	-75.682815	10.136645	2022-05-01T14:45:00
Columbia	1	MG	P9	-75.682996	10.136577	2022-05-01T14:46:00
Columbia	2	SG	P3	-75.630319	10.192668	2022-05-05T15:43:00
Columbia	2	SG	P4	-75.630338	10.192487	2022-05-05T15:39:00
Columbia	2	SG	P5	-75.630355	10.192527	2022-05-05T15:41:00
Columbia	2	UV	P1	-75.630572	10.192642	2022-05-07T15:54:00
Columbia	2	UV	P2	-75.630508	10.192592	2022-05-07T15:53:00
Columbia	2	UV	P3	-75.630435	10.192557	2022-05-07T15:52:00
Columbia	2	MG	P6	-75.630144	10.191658	2022-05-04T15:44:00
Columbia	2	MG	P3	-75.629953	10.191859	2022-05-04T15:29:00
Columbia	2	MG	P2	-75.630129	10.192157	2022-05-04T14:26:00
Columbia	3	SG	P1	-75.655608	10.171513	2022-05-08T21:21:00
Columbia	3	SG	P6	-75.655606	10.171255	2022-05-08T21:17:00
Columbia	3	UV	P1	-75.655774	10.171481	2022-05-09T14:50:00
Columbia	3	UV	P2	-75.655756	10.171415	2022-05-09T14:57:00
Columbia	3	UV	P5	-75.655592	10.171073	2022-05-09T14:56:00
Columbia	3	MG	P5	-75.655710	10.171036	2022-05-08T16:26:00
Columbia	3	MG	P6	-75.655767	10.170866	2022-05-08T16:21:00

Table S2: Porewater samples taken in North Sea, Germany: SG (seagrass), UV (unvegetated) and SM (saltmarsh). Information on sampling location, date and time.

Country	Location	Ecosystem	Point	Longitude	Latitude	Date and time
Germany	MET	UV	P8	8.965385406	54.50309346	2021-11-11T11:56:13

Germany	MET	UV	P7	8.965154674	54.50312189	2021-11-11T12:05:02
Germany	MET	UV	P6	8.964933863	54.50315194	2021-11-11T12:17:11
Germany	MET	UV	P5	8.9646673	54.50318279	2021-11-11T12:28:43
Germany	MET	UV	P4	8.964450012	54.50321822	2021-11-11T12:36:18
Germany	MET	UV	P2	8.964039088	54.50325294	2021-11-11T13:01:43
Germany	MET	UV	P1	8.963778231	54.50328101	2021-11-11T13:09:45
Germany	MET	SG	P7	8.968679146	54.50289248	2021-11-11T09:35:04
Germany	MET	SG	P6	8.968376408	54.50291868	2021-11-11T09:41:19
Germany	MET	SG	P5	8.968031533	54.50295053	2021-11-11T09:47:01
Germany	MET	SG	P3	8.967398385	54.50299082	2021-11-11T10:01:21
Germany	MET	SG	P2	8.967011384	54.50301002	2021-11-11T10:08:13
Germany	MET	SG	P1	8.966630373	54.50304336	2021-11-11T10:14:44
Germany	MET	pioneer SM	P9	8.962556616	54.50367524	2021-11-10T13:29:20
Germany	MET	pioneer SM	P8	8.962371877	54.50360048	2021-11-10T13:43:50
Germany	MET	pioneer SM	P7	8.962272025	54.50353863	2021-11-10T13:55:11
Germany	MET	low SM	P6	8.962162761	54.50347216	2021-11-10T14:04:01
Germany	MET	low SM	P5	8.962077353	54.50342044	2021-11-10T14:11:50
Germany	MET	low SM	P4	8.961963113	54.50335311	2021-11-10T14:30:54
Germany	MET	high SM	P3	8.961829112	54.50330163	2021-11-10T14:42:36
Germany	MET	high SM	P2	8.961744003	54.50327688	2021-11-10T14:49:47

Germany	MET	high SM	P1	8.961645378	54.50324664	2021-11-10T15:01:18
Germany	NES	UV	P1	7.337581152	53.68513592	2022-08-17T06:15:00
Germany	NES	UV	P2	7.337331868	53.68518217	2022-08-17T06:33:00
Germany	NES	UV	P3	7.337111836	53.68522585	2022-08-17T06:48:00
Germany	NES	UV	P4	7.336819655	53.68526396	2022-08-17T07:02:00
Germany	NES	UV	P5	7.336531409	53.68530355	2022-08-17T07:13:00
Germany	NES	UV	P6	7.336299366	53.68532768	2022-08-17T07:26:00
Germany	NES	UV	P7	7.336025374	53.6853751	2022-08-17T07:39:00
Germany	NES	UV	P9	7.335573659	53.68543607	2022-08-17T07:50:00
Germany	NES	UV	P8	7.335798533	53.68540797	2022-08-17T08:03:00
Germany	NES	SG	P1	7.336522271	53.68607174	2022-08-16T07:34:00
Germany	NES	SG	P2	7.336249798	53.68612155	2022-08-16T07:49:00
Germany	NES	SG	P3	7.336034738	53.68615325	2022-08-16T08:26:00
Germany	NES	SG	P4	7.335864038	53.68618797	2022-08-16T08:43:00
Germany	NES	SG	P5	7.335658195	53.68621189	2022-08-16T08:59:00
Germany	NES	SG	P6	7.335419068	53.68623867	2022-08-16T09:13:00
Germany	NES	SG	P7	7.335206187	53.68625372	2022-08-16T09:27:00
Germany	NES	SG	P8	7.335018737	53.68627393	2022-08-16T09:45:00
Germany	NES	SG	P9	7.334821413	53.68629682	2022-08-16T09:57:00
Germany	NES	pioneer SM	P1	7.334766191	53.6843031	2022-08-15T10:08:00

Germany	NES	pioneer SM	P2	7.335256734	53.68429143	2022-08-15T10:34:00
Germany	NES	low SM	P5	7.335258637	53.68421474	2022-08-15T10:59:00
Germany	NES	low SM	P6	7.335641285	53.68427579	2022-08-15T11:32:00

Table S3: List of tested relative antibody signal to sediment extracts with described recognized epitope and origin; adapted from (Vidal-Melgosa et al., 2021)**.**

Antibody name	Recognized epitope	Origin	Reference
BAM1	Un-sulphated epitope present in sulphated fucan	Rat	(Torode et al., 2015; SeaProbes Station Biologique de Roscoff, 2025)
BAM2	Sulphated epitope present in sulphated fucan	Rat	(Torode et al., 2015; SeaProbes Station Biologique de Roscoff, 2025)
BAM3	Possibly sulphated epitope present in sulphated fucan	Rat	(Torode et al., 2015; SeaProbes Station Biologique de Roscoff, 2025)
BAM4	Sulphated epitope present in sulphated fucan	Rat	(Torode et al., 2015; SeaProbes Station Biologique de Roscoff, 2025)
JIM5	Partially methyl-esterified/de-esterified HG	Rat	(Clausen et al., 2003)
JIM7	Partially methyl-esterified HG	Rat	(Clausen et al., 2003)
LM18	Partially methyl-esterified/de-esterified HG	Rat	(Verhertbruggen et al., 2009)
LM19	Partially methyl-esterified/de-esterified HG	Rat	(Verhertbruggen et al., 2009)
LM20	Partially methyl-esterified HG	Rat	(Verhertbruggen et al., 2009)
LM7	Non-blockwise partially methyl-esterified HG	Rat	(Willats et al., 2001)
LM8	Xylogalacturonan	Rat	(Willats et al., 2004)
INRA-RU2	Rhamnogalacturonan I backbone	Mouse	(Ralet et al., 2010)
INRA-RU1	Rhamnogalacturonan I backbone	Mouse	(Ralet et al., 2010)
LM13	Linearised (1→5)-α-L-arabinan	Rat	(Verhertbruggen et al., 2009)
LM16	Rhamnogalacturonan I arabinosyl side chains	Rat	(Verhertbruggen et al., 2009)
LM5	(1→4)-β-D-galactan	Rat	(Jones and Knox, 1997)
LM6	(1→5)-α-L-arabinan	Rat	(Willats et al., 1998)
LM6-M	(1→5)-α-L-arabinan	Rat	(Cornuault et al., 2017)
CBM3a	Cellulose	His	(Blake et al., 2006)
BS-400-2	(1→3)-β-D-glucan	Mouse	(Meikle et al., 1991)
BS-400-3	(1→3)(1→4)-β-D-glucan	Mouse	(Meikle et al., 1994)
BS-400-4	(1→4)-β-D-(galacto)(gluco)mannan	Mouse	(Pettolino et al., 2001)
LM21	(1→4)-β-D-(galacto)(gluco)mannan	Rat	(Marcus et al., 2010)
LM22	(1→4)-β-D-(galacto)(gluco)mannan	Rat	(Marcus et al., 2010)
LM15	Xyloglucan (XXXG motif)	Rat	(Marcus et al., 2008)
LM25	Xyloglucan (XXXG motif, both galactosylated and non-galactosylated)	Rat	(Pedersen et al., 2012)

LM26	branched (1,6-Gal) (1→4)-β-D-galactan	Rat	(Posé et al., 2018)
LM28	Glucuronoxylan	Rat	(Cornuault et al., 2015)
LM30	Arabinogalactan protein glycan	Rat	(Sanhueza et al., 2024)
LM10	(1→4)-β-D-xylan	Rat	(McCartney et al., 2005)
LM11	(1→4)-β-D-xylan/arabinoxylan	Rat	(McCartney et al., 2005)
INRA-AX1	(1→4)-β-D-xylan/arabinoxylan	Mouse	(Guillon et al., 2004)
LM23	Xylosyl residues	Rat	(Pedersen et al., 2012)
LM24	Galactosylated Xyloglucan	Rat	(Pedersen et al., 2012)
LM27	unknown epitope associated with grass xylan	Rat	(Cornuault et al., 2015)
JIM19	Extensin	Rat	(Knox et al., 1995)
JIM4	Arabinogalactan protein glycan	Rat	(Knox et al., 1989)
JIM8	Arabinogalactan protein glycan	Rat	(Pennell et al., 1991)
JIM13	Arabinogalactan protein glycan	Rat	(Knox et al., 1991)
JIM15	Arabinogalactan protein glycan	Rat	(Knox et al., 1991)
JIM16	Arabinogalactan protein glycan	Rat	(Knox et al., 1991)
JIM20	Extensin	Rat	(Smallwood et al., 1994)
LM1	Extensin	Rat	(Smallwood et al., 1995)
LM2	β-linked GlcA in arabinogalactan protein	Rat	(Yates et al., 1996)
LM12	Feruloylated polymers	Rat	(Pedersen et al., 2012)
LM14	GlcA in arabinogalactan protein	Rat	(Moller et al., 2008; Pedersen et al., 2012)
MAC207	Arabinogalactan protein glycan	Rat	(Pennell et al., 1989)
BAM6	Alginate - mannuronate-rich epitope	Rat	(Torode et al., 2016; SeaProbes Station Biologique de Roscoff, 2025)
BAM7	Alginate - mannuronate-guluronate	Rat	(Torode et al., 2016; SeaProbes Station Biologique de Roscoff, 2025)
BAM8	Alginate - mannuronate-guluronate	Rat	(Torode et al., 2016; SeaProbes Station Biologique de Roscoff, 2025)
BAM9	Alginate - mannuronate-guluronate	Rat	(Torode et al., 2016; SeaProbes Station Biologique de Roscoff, 2025)
BAM10	Alginate - mannuronate-guluronate	Rat	(Torode et al., 2016; SeaProbes Station Biologique de Roscoff, 2025)
BAM11	Alginate - ~7 guluronate residues	Rat	(Torode et al., 2016; SeaProbes Station Biologique de Roscoff, 2025)
JIM11	Extensin	Rat	(Smallwood et al., 1994)
JIM12	Extensin	Rat	(Smallwood et al., 1994)
JIM14	Arabinogalactan protein glycan	Rat	(Knox et al., 1991)

S1.2 Supplementary figures

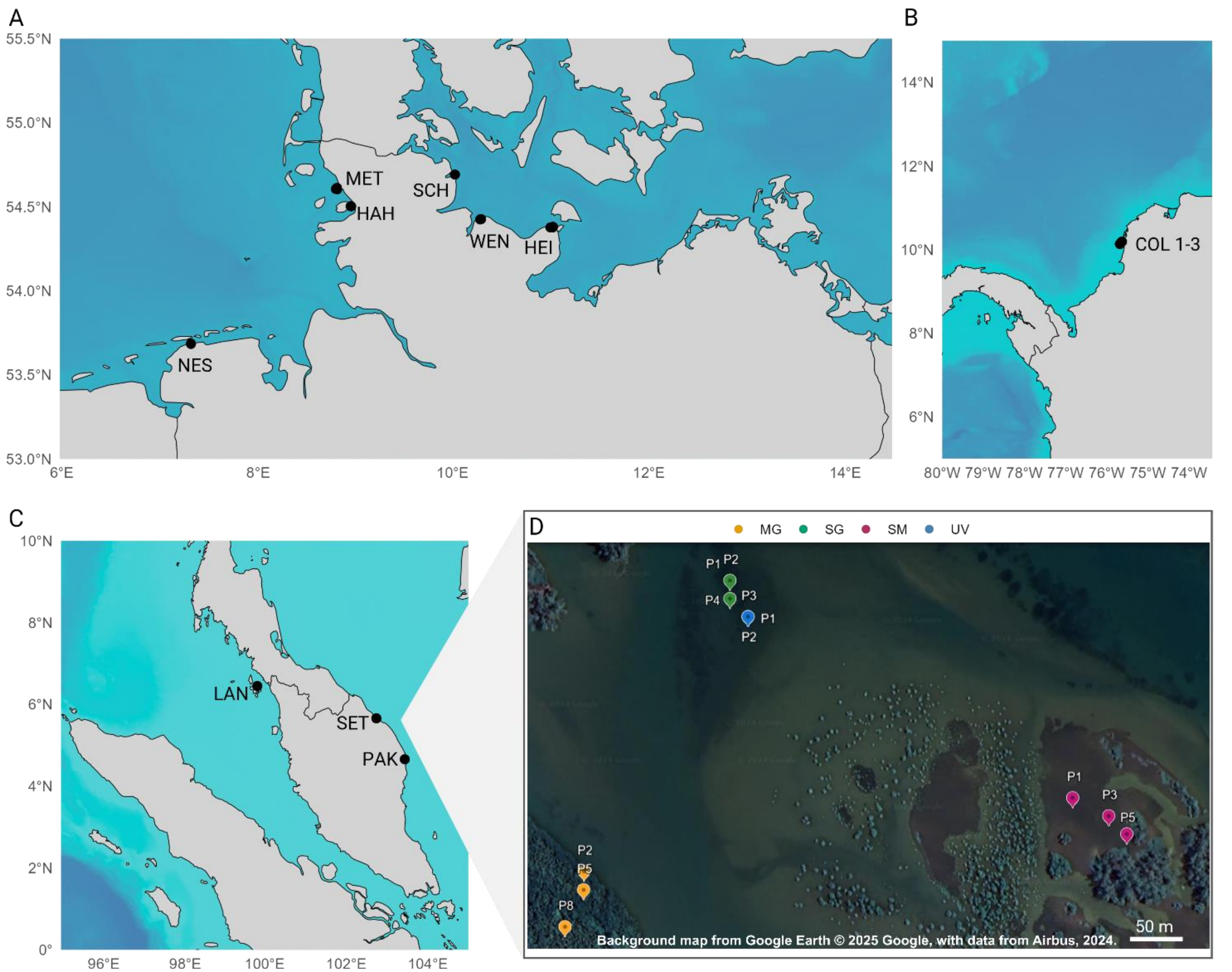

Fig.S1: Global sampling map of sediment cores of coastal vegetated ecosystems. Bathymetrie is increasing with darker blue scale, bathymetry data is from NOAA (2022), plotted with R packages 'marmap' (Pante and Simon-Bouhet, 2013) and 'sf' (Bivand, 2021). **A)** Sampling locations along the North and Baltic Sea, Germany. NES: Nessmersiel, HAH: Hamburger Hallig, MET: Mettgrund, SCH: Schleimünde, WEN: Wendtorf, HEI: Heiligenhafen, **B)** in Columbia: COL sites 1 to 3 and **C)** in Malaysia, LAN: Langkawi, SET: Setiu, PAK: Paka. **D)** Example transect map, plotted with QGIS 3.22, of analysed transect point in ecosystems sampled in Setiu, Malaysia: mangroves (yellow), seagrass (green), saltmarsh (maroon), unvegetated (blue). Further information on analysed sampling points with locations are shown in supplementary **table S1**.

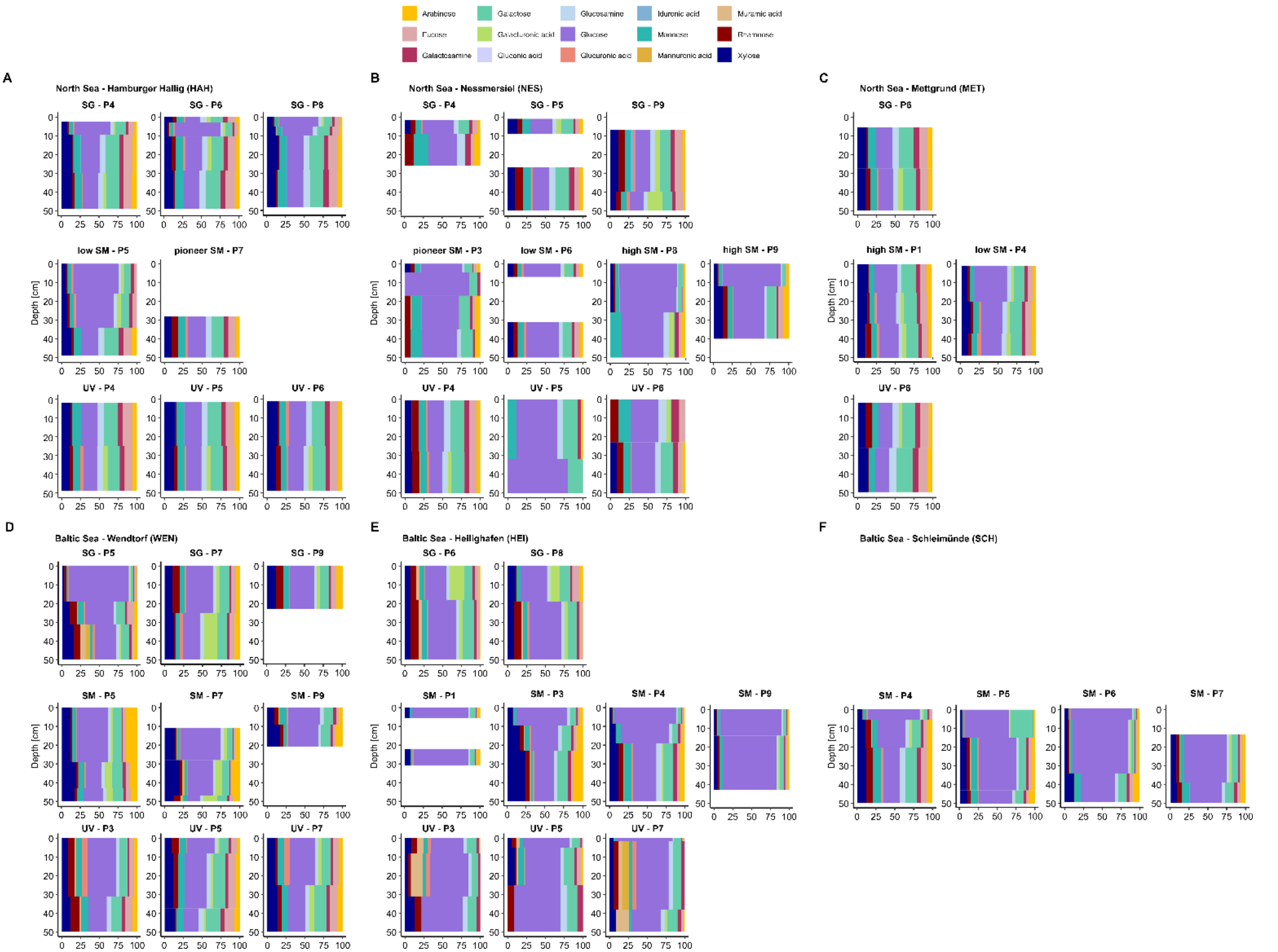

Fig. S2: Relative abundances of monosaccharides in sediment cores in Germany, shown by sampling site and point and ecosystems (SG: seagrass, SM: saltmarsh, UV: unvegetated ecosystems). Sediment cores were split visually according to visible physicochemical layers, represented by depth in cm. **A)** Sampling at Hamburger Hallig (HAH), North Sea site; **B)** Nessmersiel (NES), North Sea site; **C)** Mettgrund (MET), North Sea site; **D)** Wendtorf (WEN), Baltic Sea; **E)** Heiligenhafen (HEI), Baltic Sea; **F)** Schleimünde (SCH), Baltic Sea.

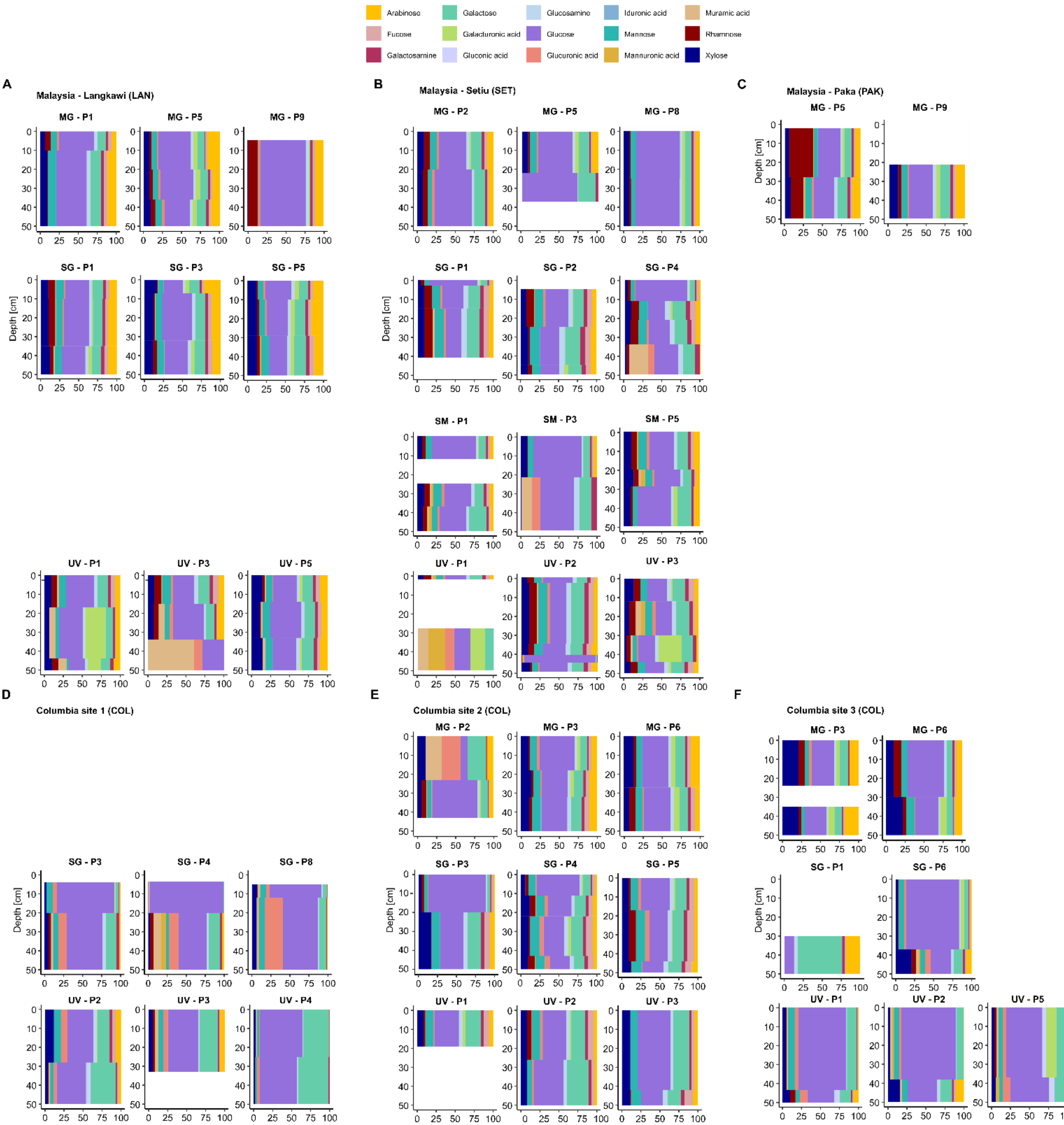

Fig. S3: Relative abundances of monosaccharides in sediment cores in Malaysia and Columbia, shown by sampling site and point and ecosystems (SG: seagrass, SM: saltmarsh, UV: unvegetated ecosystems). Sediment cores were split visually according to visible physicochemical layers, represented by depth in cm. **A)** Langkawi (LAN), Malaysia; **B)** Setiu (SET), Malaysia; **C)** Paka (PAK), Malaysia; **D)** Columbia site 1 (COL), **E)** Columbia site 2 (COL), **F)** Columbia site 3 (COL). COL1 mangroves cores sampled and analyzed, but due to missing depths abundance cannot be displayed.

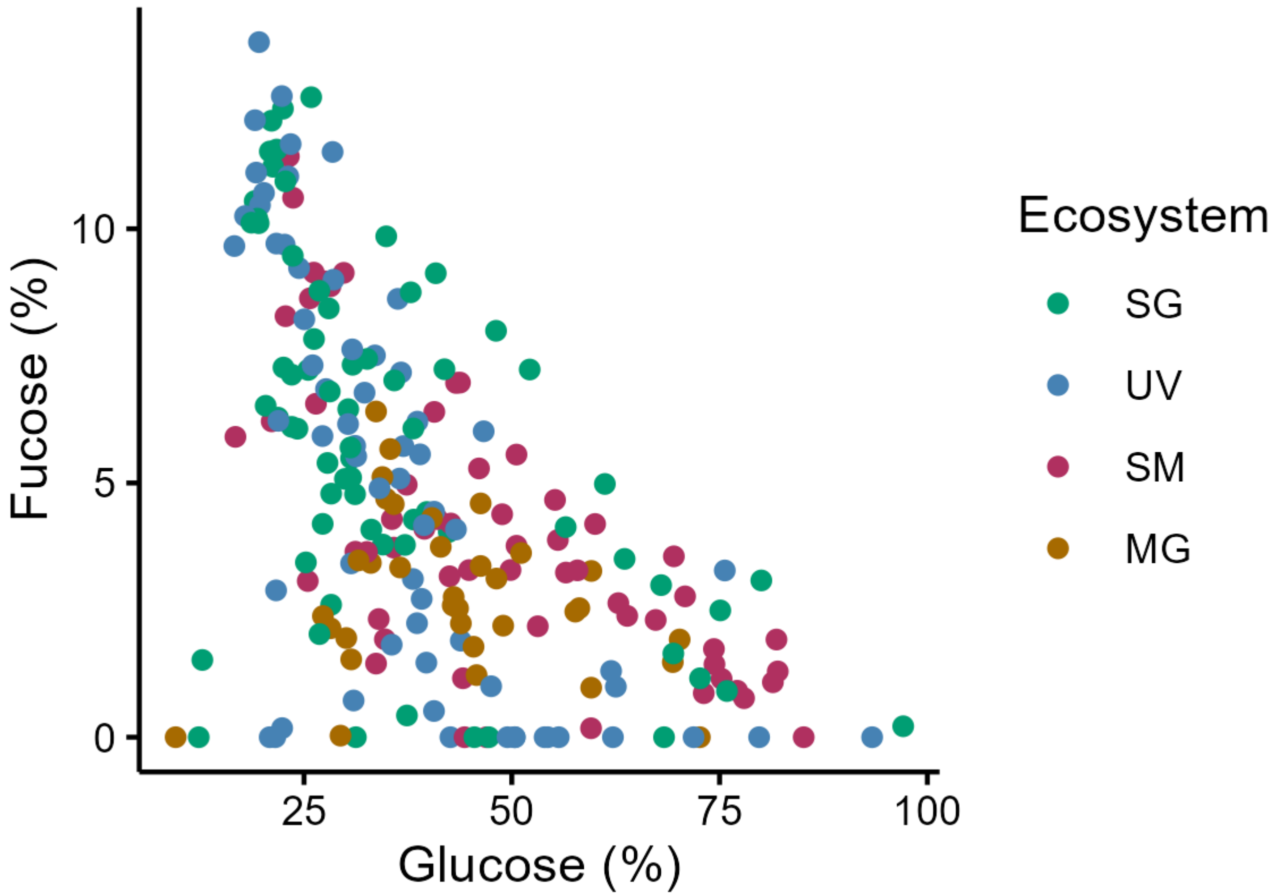

Fig. S4: The direct relationship between the relative abundance of the two monosaccharides fucose and glucose for all ecosystems: SG: seagrass, UV: unvegetated areas, SM: saltmarsh areas and MG: mangroves.

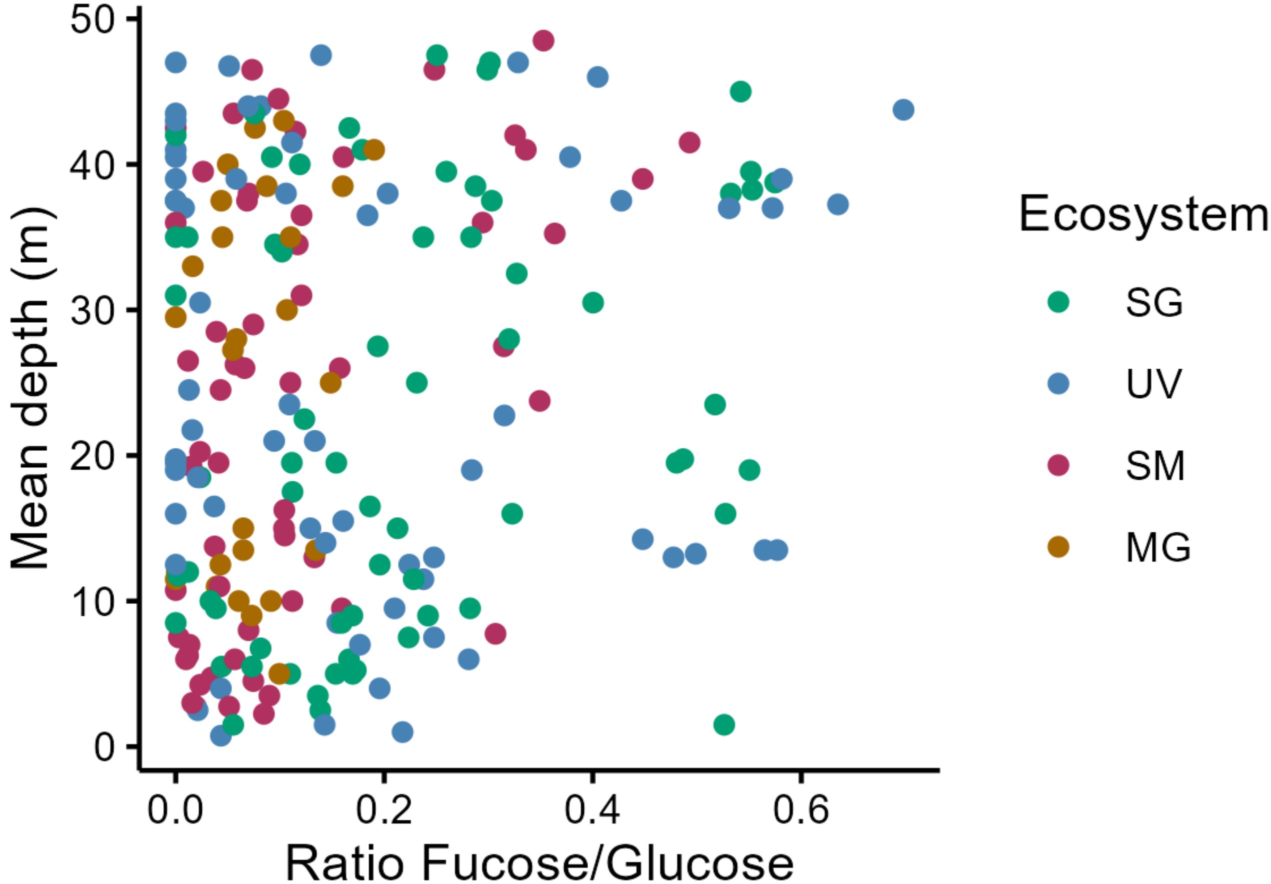

Fig. S5: Relationship of mean depth in m and fucose/glucose ratio for all ecosystems: SG: seagrass, UV: unvegetated areas, SM: saltmarsh areas and MG: mangroves.

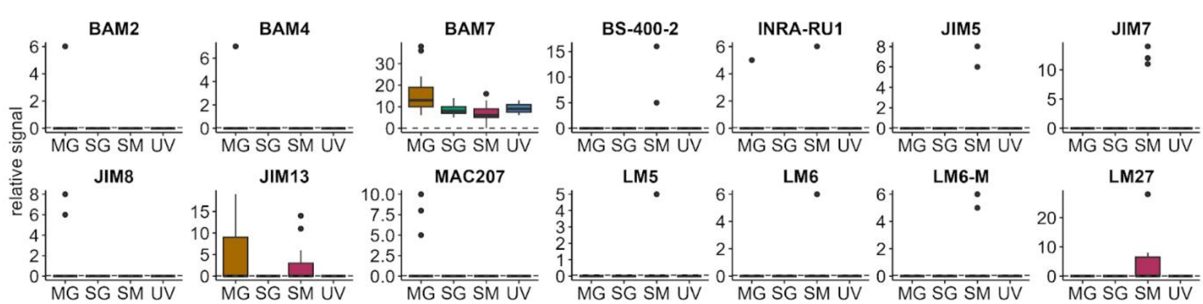

Fig. S6: Microarray antibody binding revealed presence of alginate, fucoidan, pectin, grass xylan and arabinogalactan. Only antibodies that exhibited a clear relative signal were included in the analysis; BAM1 was excluded due to scattered signals. Binding to BAM2 and BAM4 (sulfated epitope in sulfated fucan), BAM7 (alginate -pectin or fucoidan), BS400-2

((1→3)-β-D-glucan), INRA-RU1 (rhamnogalacturonan I backbone), JIM5 (partially methyl-esterified/de-esterified HG), JIM7 (methyl-esterified HG), JIM8, JIM13 and MAC207 (all arabinogalactan protein glycan), LM5 ((1→4)-β-D-galactan), LM6 ((1→5)-α-L-arabinan; recognizes short arabinan chains (Cornuault et al., 2014), LM6-M ((1→5)-α-L-arabinan; recognizes longer arabinan chains (Cornuault et al., 2017)), LM27 (grass-xylan).

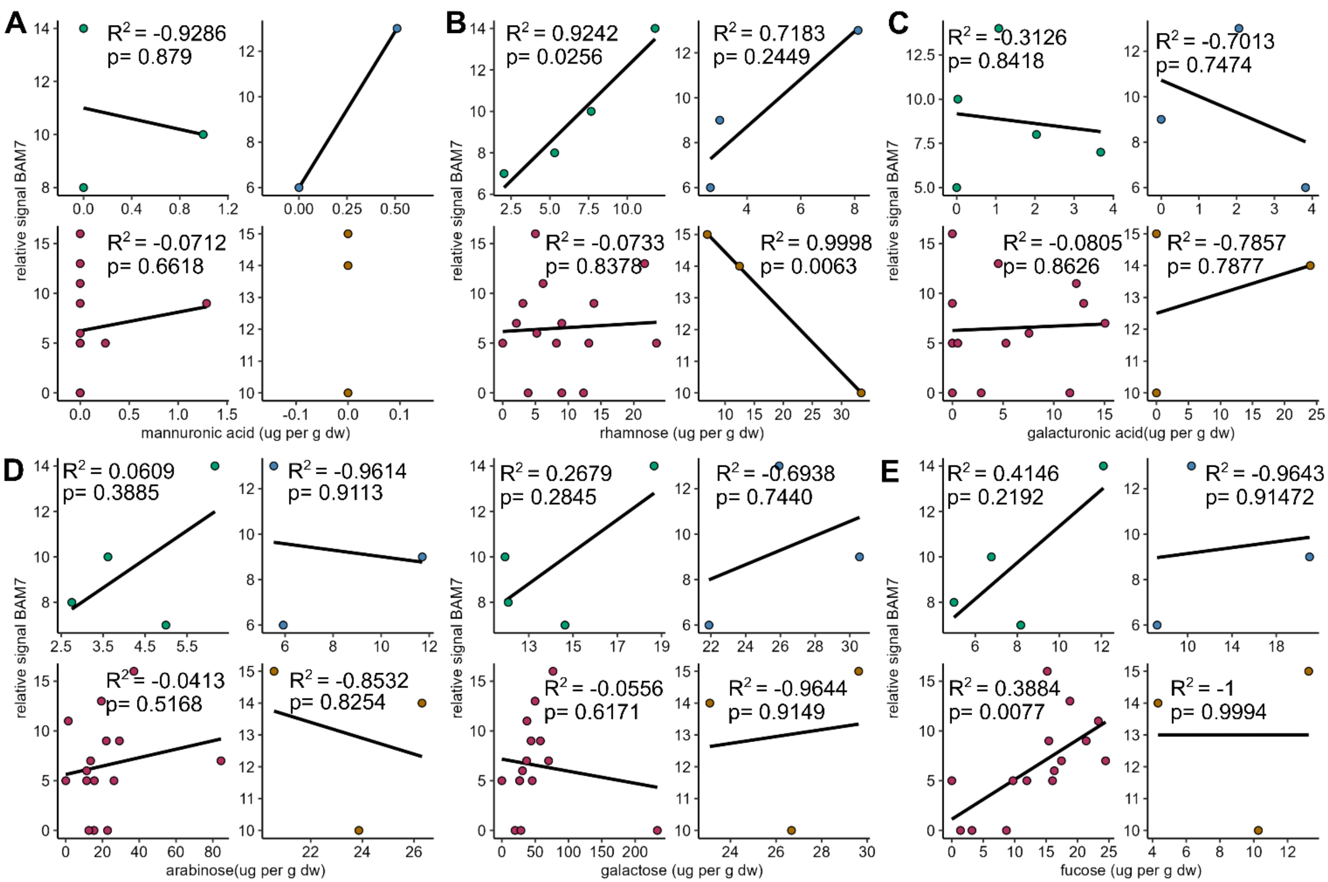

Fig. S7: Tested correlation of relative BAM7 signals to the main monosaccharides of alginate, pectin and fucoidan. Monosaccharide concentrations derived from monosaccharide analysis in ug g_{dw}^{-1} (dw: dry weight). **A)** No correlation between BAM7 signal and mannuronic acid concentrations, one of the main monosaccharides of alginate. **B)** BAM7 signal correlates to rhamnose concentrations in seagrass ecosystem and unvegetated areas. Correlation to rhamnose might hint towards presence of pectin **C)** No correlation between BAM7 signal and galacturonic acid concentrations for all ecosystems. **D)** No correlation between BAM7 signal and arabinose concentrations for all ecosystems. **E)** No correlation between BAM7 signal and galactose concentrations for all ecosystems. **F)** Slight correlation of BAM7 signal to fucose concentrations in seagrass and saltmarsh areas; might hint towards presence of fucoidan.

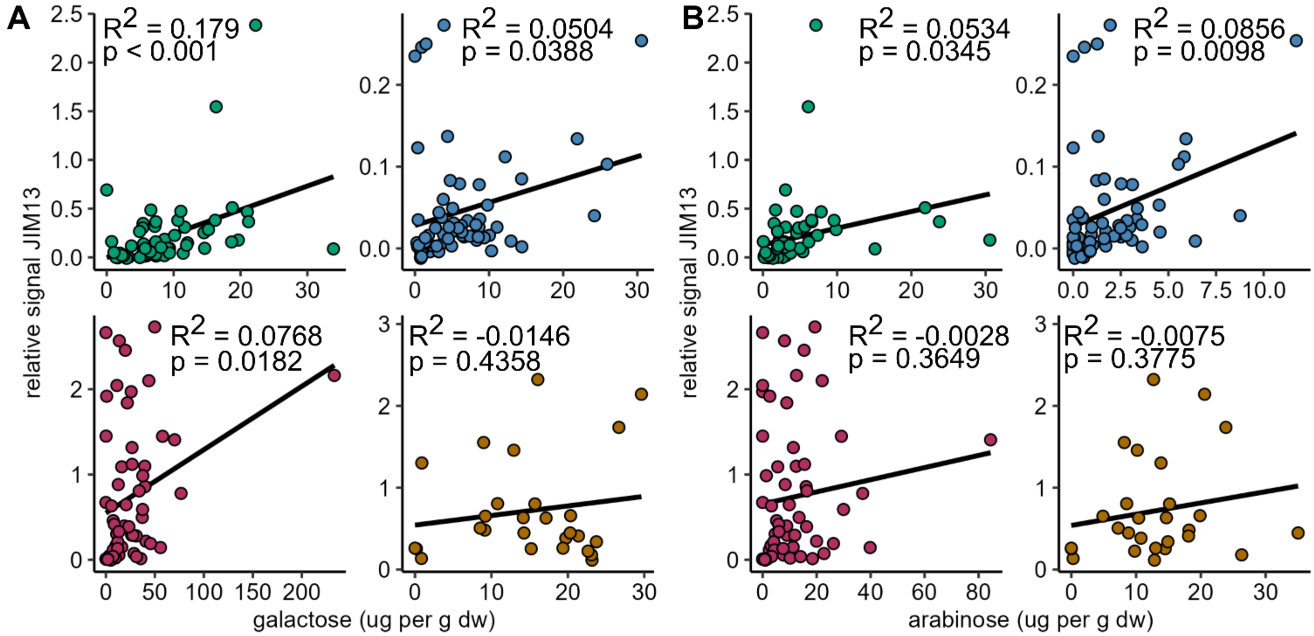

Fig. S8: Relative JIM13 signal does not correlate with **A)** galactose or **B)** arabinose concentrations derived from monosaccharide analysis in ug g_{dw}^{-1} (dw: dry weight). Weak correlation of relative JIM13 signal to galactose in seagrass ecosystems.

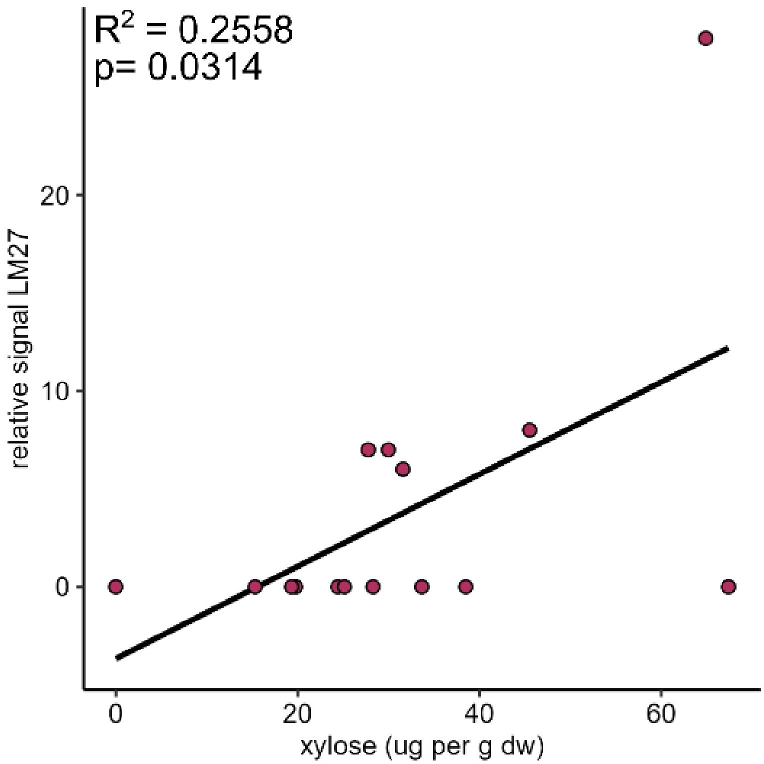

Fig. S9: Relative LM27 signal correlates weakly with xylose concentrations derived from monosaccharide analysis in ug g_{dw}^{-1} (dw: dry weight). No LM27 signal for other ecosystems detected.

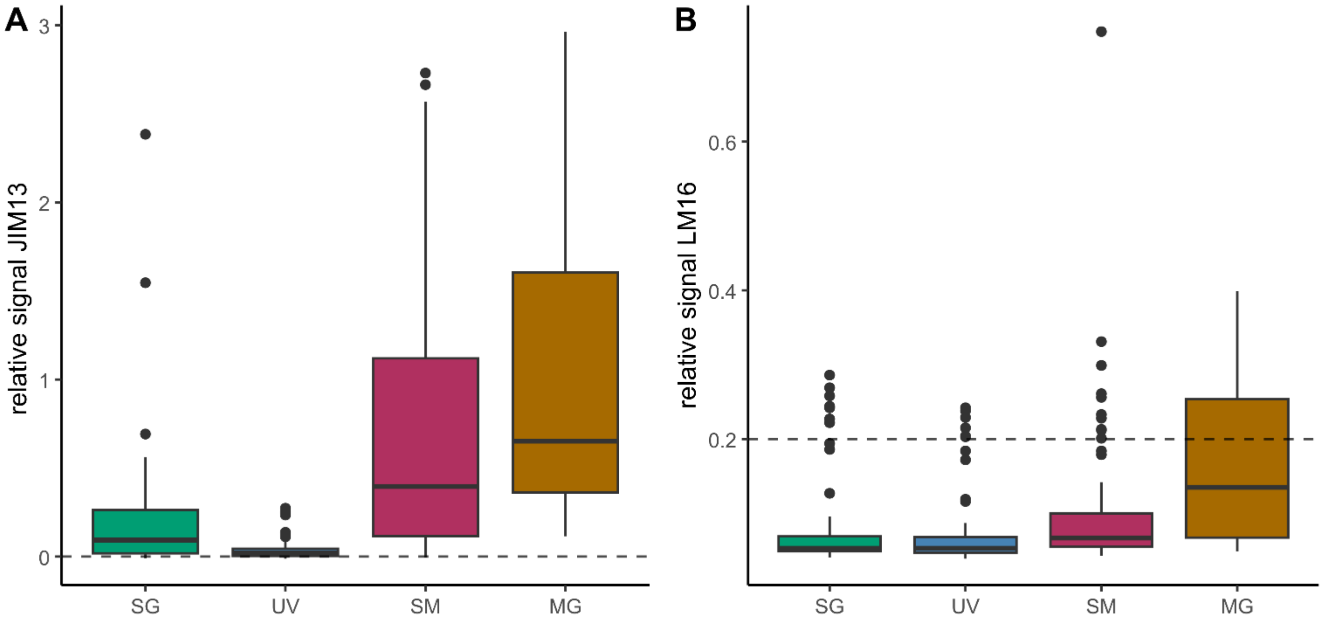

Fig. S10: Relative antibody signal of JIM13 and LM16 normalized to MilliQ-blank (dashed line), representing arabinogalactans and pectins using ELISA method. **A)** Arabinogalactans (JIM13) found in saltmarsh (SM), mangrove (MG) and seagrass (SG) areas. No signal in unvegetated areas (UV). **B)** High signal in background MilliQ-blank signal. Comparable no singal for pectins in coastal vegetated ecosystems.

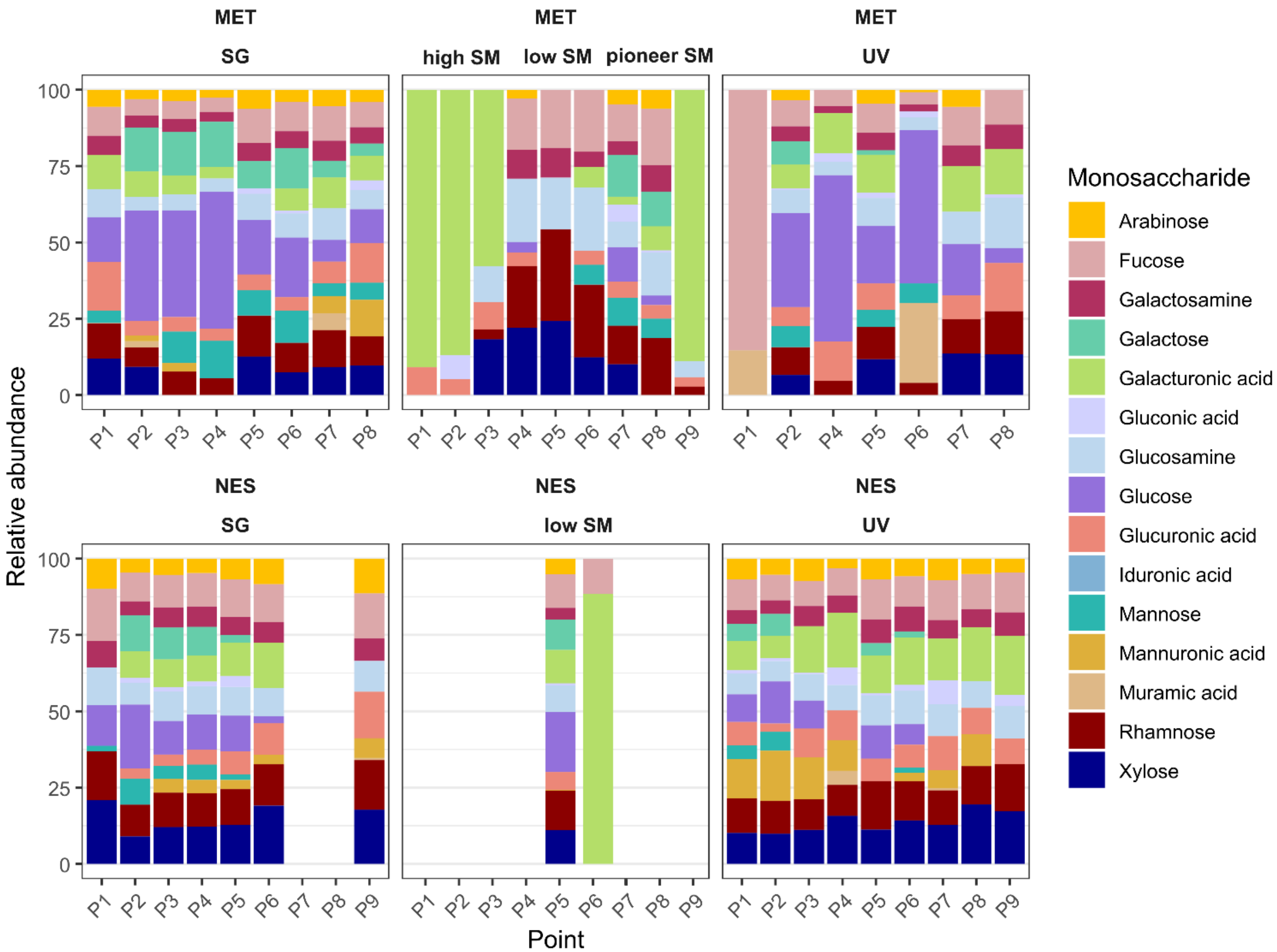

85

Fig. S11: Relative abundances of monosaccharides in porewater samples for two sites in the North Sea. Samples were taken in Mettgrund (MET) and Nessmersiel (NES), relative monosaccharide abundances are shown for each sampling point and ecosystems (SG: seagrass, SM: saltmarsh, UV: unvegetated ecosystems). The SM sites can be divided into a clear zonation by vegetation and are divided into high, low and pioneer SM.

90

References

Bivand, R. S.: Progress in the R ecosystem for representing and handling spatial data, J Geogr Syst, 23, 515–546, https://doi.org/10.1007/s10109-020-00336-0, 2021.

Blake, A. W., McCartney, L., Flint, J. E., Bolam, D. N., Boraston, A. B., Gilbert, H. J., and Knox, J. P.: Understanding the Biological Rationale for the Diversity of Cellulose-directed Carbohydrate-binding Modules in Prokaryotic Enzymes, Journal of Biological Chemistry, 281, 29321–29329, https://doi.org/10.1074/jbc.M605903200, 2006.

Clausen, M. H., Willats, W. G. T., and Knox, J. P.: Synthetic methyl hexagalacturonate hapten inhibitors of anti-homogalacturonan monoclonal antibodies LM7, JIM5 and JIM7, Carbohydrate Research, 338, 1797–1800, https://doi.org/10.1016/S0008-6215(03)00272-6, 2003.

Cornuault, V., Manfield, I. W., Ralet, M., and Knox, J. P.: Epitope detection chromatography: a method to dissect the structural heterogeneity and inter-connections of plant cell-wall matrix glycans, The Plant Journal, 78, 715–722, https://doi.org/10.1111/tpj.12504, 2014.

Cornuault, V., Buffetto, F., Rydahl, M. G., Marcus, S. E., Torode, T. A., Xue, J., Crépeau, M.-J., Faria-Blanc, N., Willats, W. G. T., Dupree, P., Ralet, M.-C., and Knox, J. P.: Monoclonal antibodies indicate low-abundance links between heteroxylan and other glycans of plant cell walls, Planta, 242, 1321–1334, https://doi.org/10.1007/s00425-015-2375-4, 2015.

Cornuault, V., Buffetto, F., Marcus, S. E., Crépeau, M.-J., Guillon, F., Ralet, M.-C., and Knox, J. P.: LM6-M: a high avidity rat monoclonal antibody to pectic α-1,5-L-arabinan, https://doi.org/10.1101/161604, 10 July 2017.

Guillon, F., Tranquet, O., Quillien, L., Utille, J.-P., Ordaz Ortiz, J. J., and Saulnier, L.: Generation of polyclonal and monoclonal antibodies against arabinoxylans and their use for immunocytochemical location of arabinoxylans in cell walls of endosperm of wheat, Journal of Cereal Science, 40, 167–182, https://doi.org/10.1016/j.jcs.2004.06.004, 2004.

Jones, L. and Knox, J. P.: Localization of Pectic Galactan in Tomato Cell Walls Usinga Monoclonal Antibody Specific to (1--+4)-P-~-Galactan', 1997.

Knox, J., Peart, J., and Neill, StevenJ.: Identification of novel cell surface epitopes using a leaf epidermal-strip assay system, Planta, 196, https://doi.org/10.1007/BF00201383, 1995.

Knox, J. P., Day, S., and Roberts, K.: A set of cell surface glycoproteins forms an early marker of cell position, but not cell type, in the root apical meristem of *Daucus carota* L., Development, 106, 47–56, https://doi.org/10.1242/dev.106.1.47, 1989.

Knox, J. P., Linstead, P. J., Cooper, J. P., C., and Roberts, K.: Developmentally regulated epitopes of cell surface arabinogalactan proteins and their relation to root tissue pattern formation, The Plant Journal, 1, 317–326, https://doi.org/10.1046/j.1365-313X.1991.t01-9-00999.x, 1991.

Marcus, S. E., Verhertbruggen, Y., Hervé, C., Ordaz-Ortiz, J. J., Farkas, V., Pedersen, H. L., Willats, W. G., and Knox, J. P.: Pectic homogalacturonan masks abundant sets of xyloglucan epitopes in plant cell walls, BMC Plant Biol, 8, 60, https://doi.org/10.1186/1471-2229-8-60, 2008.

Marcus, S. E., Blake, A. W., Benians, T. A. S., Lee, K. J. D., Poyser, C., Donaldson, L., Leroux, O., Rogowski, A., Petersen, H. L., Boraston, A., Gilbert, H. J., Willats, W. G. T., and Paul Knox, J.: Restricted access of proteins to mannan polysaccharides in intact plant cell walls: Masking of mannan polysaccharides, The Plant Journal, 64, 191–203, https://doi.org/10.1111/j.1365-313X.2010.04319.x, 2010.

McCartney, L., Marcus, S. E., and Knox, J. P.: Monoclonal Antibodies to Plant Cell Wall Xylans and Arabinoxylans, J Histochem Cytochem., 53, 543–546, https://doi.org/10.1369/jhc.4B6578.2005, 2005.

Meikle, P. J., Bonig, I., Hoogenraad, N. J., Clarke, A. E., and Stone, B. A.: The location of (1--, 3)-fl-glucans in the walls of pollen tubes of Nicotiana alata using a (1 3)-fl-glucan-specific monoclonal antibody, 1991.

Meikle, P. J., Hoogenraad, N. J., Bonig, I., Clarke, A. E., and Stone, B. A.: A (1→3,1→4)-β-glucan-specific monoclonal antibody and its use in the quantitation and immunocytochemical location of (1→3,1→4)-β-glucans, The Plant Journal, 5, 1–9, https://doi.org/10.1046/j.1365-313X.1994.5010001.x, 1994.

Moller, I., Marcus, S. E., Haeger, A., Verhertbruggen, Y., Verhoef, R., Schols, H., Ulvskov, P., Mikkelsen, J. D., Knox, J. P., and Willats, W.: High-throughput screening of monoclonal antibodies against plant cell wall glycans by hierarchical clustering of their carbohydrate microarray binding profiles, Glycoconj J, 25, 37–48, https://doi.org/10.1007/s10719-007-9059-7, 2008.

Pante, E. and Simon-Bouhet, B.: marmap: A Package for Importing, Plotting and Analyzing Bathymetric and Topographic Data in R, PLoS ONE, 8, e73051, https://doi.org/10.1371/journal.pone.0073051, 2013.

Pedersen, H. L., Fangel, J. U., McCleary, B., Ruzanski, C., Rydahl, M. G., Ralet, M.-C., Farkas, V., Von Schantz, L., Marcus, S. E., Andersen, M. C. F., Field, R., Ohlin, M., Knox, J. P., Clausen, M. H., and Willats, W. G. T.: Versatile High Resolution Oligosaccharide Microarrays for Plant Glycobiology and Cell Wall Research, Journal of Biological Chemistry, 287, 39429–39438, https://doi.org/10.1074/jbc.M112.396598, 2012.

Pennell, R. I., Knox, J. P., Scofield, G. N., Selvendran, R. R., and Roberts, K.: A family of abundant plasma membrane-associated glycoproteins related to the arabinogalactan proteins is unique to flowering plants., The Journal of cell biology, 108, 1967–1977, https://doi.org/10.1083/jcb.108.5.1967, 1989.

Pennell, R. I., Janniche, L., Kjellbom, P., Scofield, G. N., Peart, J. M., and Roberts, K.: Developmental Regulation of a Plasma Membrane Arabinogalactan Protein Epitope in Oilseed Rape Flowers., Plant Cell, 1317–1326, https://doi.org/10.1105/tpc.3.12.1317, 1991.

Pettolino, F. A., Hoogenraad, N. J., Ferguson, C., Bacic, A., Johnson, E., and Stone, B. A.: A (1→4)-β-mannan-specific monoclonal antibody and its use in the immunocytochemical location of galactomannans, Planta, 214, 235–242, https://doi.org/10.1007/s004250100606, 2001.

Posé, S., Marcus, S. E., and Knox, J. P.: Differential metabolism of pectic galactan in tomato and strawberry fruit: detection of the LM26 branched galactan epitope in ripe strawberry fruit, Physiologia Plantarum, 164, 95–105, https://doi.org/10.1111/ppl.12748, 2018.

Ralet, M.-C., Tranquet, O., Poulain, D., Moïse, A., and Guillon, F.: Monoclonal antibodies to rhamnogalacturonan I backbone, Planta, 231, 1373–1383, https://doi.org/10.1007/s00425-010-1116-y, 2010.

Sanhueza, D., Sepúlveda-Orellana, P., Salazar-Carrasco, A., Zúñiga, S., Herrera, R., Moya-León, M. A., and Saez-Aguayo, S.: Mucilage extracted from Chilean papaya seeds is enriched with homogalacturonan domains, Front. Plant Sci., 15, 1380533, https://doi.org/10.3389/fpls.2024.1380533, 2024.

SeaProbes | Core Facilities | Station Biologique de Roscoff: https://www.sb-roscoff.fr/en/seaprobes, last access: 4 December 2025.

Smallwood, M., Beven, A., Donovan, N., Neill, S. J., Peart, J., Roberts, K., and Knox, J. P.: Localization of cell wall proteins in relation to the developmental anatomy of the carrot root apex, The Plant Journal, 5, 237–246, https://doi.org/10.1046/j.1365-313X.1994.05020237.x, 1994.

Smallwood, M., Martin, H., and Knox, J. P.: An epitope of rice threonine- and hydroxyproline-rich glycoprotein is common to cell wall and hydrophobic plasma-membrane glycoproteins, Planta, 196, https://doi.org/10.1007/BF00203651, 1995.

Torode, T. A., Marcus, S. E., Jam, M., Tonon, T., Blackburn, R. S., Hervé, C., and Knox, J. P.: Monoclonal Antibodies Directed to Fucoidan Preparations from Brown Algae, PLoS ONE, 10, e0118366, https://doi.org/10.1371/journal.pone.0118366, 2015.

Torode, T. A., Siméon, A., Marcus, S. E., Jam, M., Le Moigne, M.-A., Duffieux, D., Knox, J. P., and Hervé, C.: Dynamics of cell wall assembly during early embryogenesis in the brown alga *Fucus*, EXBOTJ, 67, 6089–6100, https://doi.org/10.1093/jxb/erw369, 2016.

Verhertbruggen, Y., Marcus, S. E., Haeger, A., Ordaz-Ortiz, J. J., and Knox, J. P.: An extended set of monoclonal antibodies to pectic homogalacturonan, Carbohydrate Research, 344, 1858–1862, https://doi.org/10.1016/j.carres.2008.11.010, 2009.

Vidal-Melgosa, S., Sichert, A., Francis, T. B., Bartosik, D., Niggemann, J., Wichels, A., Willats, W. G. T., Fuchs, B. M., Teeling, H., Becher, D., Schweder, T., Amann, R., and Hehemann, J.-H.: Diatom fucan polysaccharide precipitates carbon during algal blooms, Nat Commun, 12, 1150, https://doi.org/10.1038/s41467-021-21009-6, 2021.

Willats, W. G. T., Marcus, S. E., and Knox, J. P.: Generation of a monoclonal antibody speciÆc to (1!5)- -l-arabinan, 1998.

Willats, W. G. T., Orfila, C., Limberg, G., Buchholt, H. C., Van Alebeek, G.-J. W. M., Voragen, A. G. ., Marcus, S. E., Christensen, T. M. I. E., Mikkelsen, J. D., Murray, B. S., and Knox, J. P.: Modulation of the Degree and Pattern of Methyl-esterification of Pectic Homogalacturonan in Plant Cell Walls, Journal of Biological Chemistry, 276, 19404–19413, https://doi.org/10.1074/jbc.M011242200, 2001.

Willats, W. G. T., McCartney, L., Steele-King, C. G., Marcus, S. E., Mort, A., Huisman, M., Van Alebeek, G.-J., Schols, H. A., Voragen, A. G. J., Le Goff, A., Bonnin, E., Thibault, J.-F., and Knox, J. P.: A xylogalacturonan epitope is specifically associated with plant cell detachment, Planta, 218, 673–681, https://doi.org/10.1007/s00425-003-1147-8, 2004.

Yates, E. A., Valdor, J.-F., Haslam, S. M., Morris, H. R., Dell, A., Mackie, W., and Knox, J. P.: Characterization of carbohydrate structural features recognized by anti-arabinogalactan-protein monoclonal antibodies, Glycobiology, 6, 131–139, https://doi.org/10.1093/glycob/6.2.131, 1996.